

# **Thermal evaporation as sample preparation for silver-assisted laser desorption/ionization mass spectrometry imaging of cholesterol in amyloid tissues**

Štěpán Strnad<sup>a</sup>, Vladimír Vrkoslav<sup>a</sup>, Anna Mengr<sup>a</sup>, Ondřej Fabián<sup>b,c</sup>, Jiří Rybáček<sup>a</sup>, Miloš Kubánek<sup>b</sup>, Vojtěch Melenovský<sup>b</sup>, Lenka Maletínská<sup>a</sup>, Josef Cvačka<sup>a</sup>

<sup>a</sup> Institute of Organic Chemistry and Biochemistry of the Czech Academy of Sciences, 166 10, Prague, Czech Republic

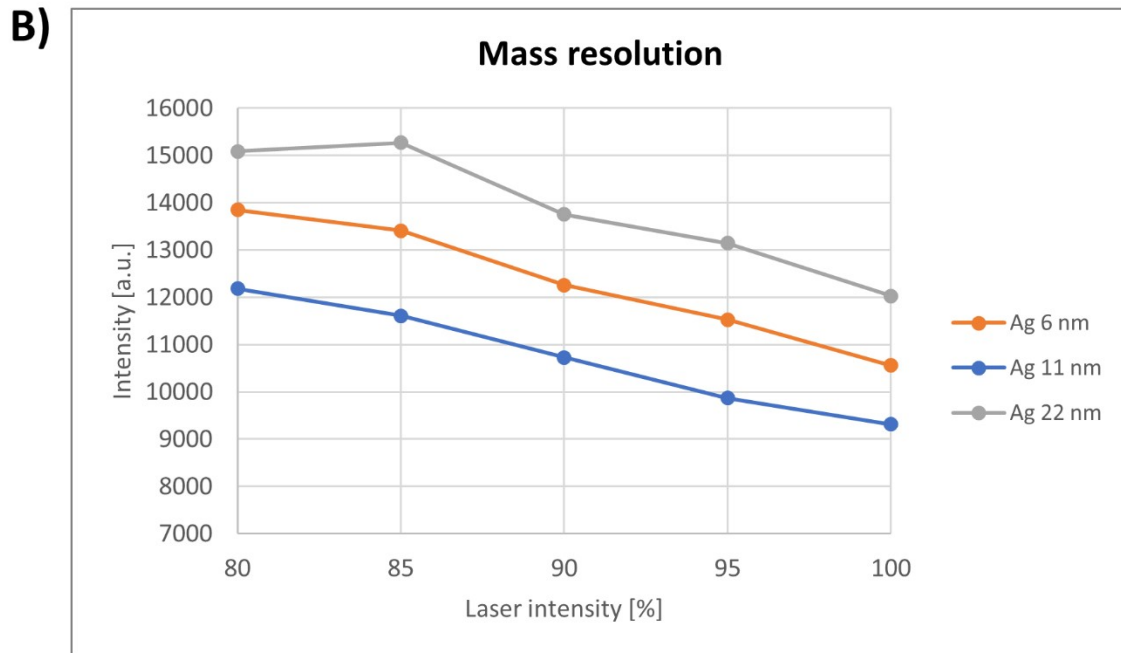
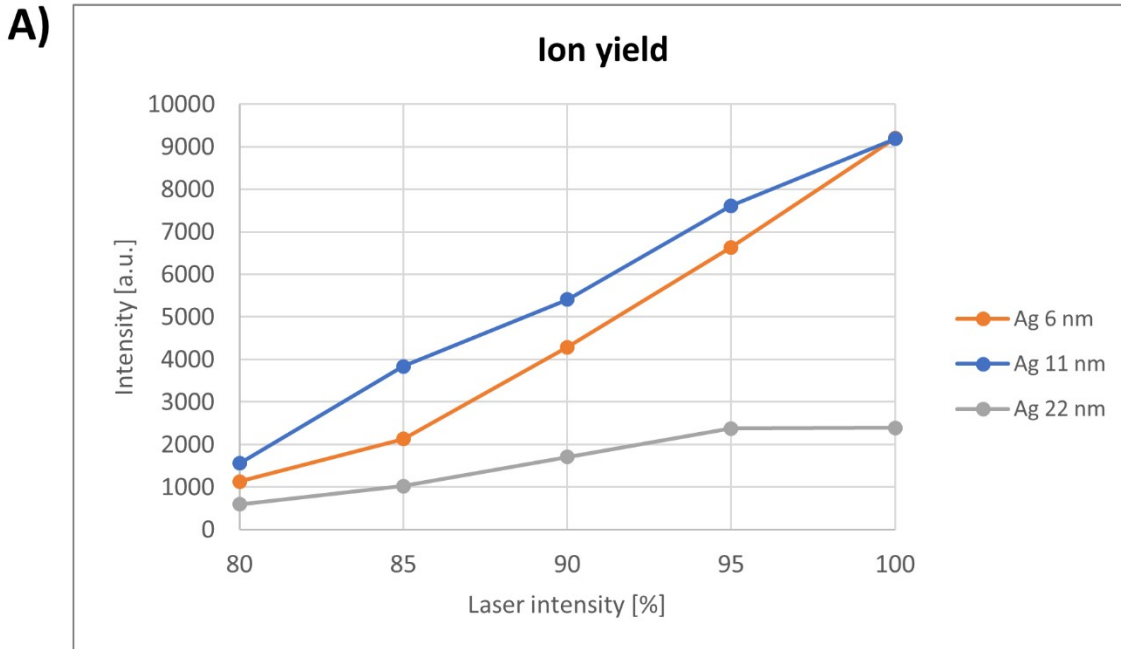
<sup>b</sup> Institute for Clinical and Experimental Medicine, 140 21, Prague, Czech Republic

<sup>c</sup> Department of Pathology and Molecular Medicine, Third Faculty of Medicine, Charles University and Thomayer Hospital, 140 59, Prague, Czech Republic

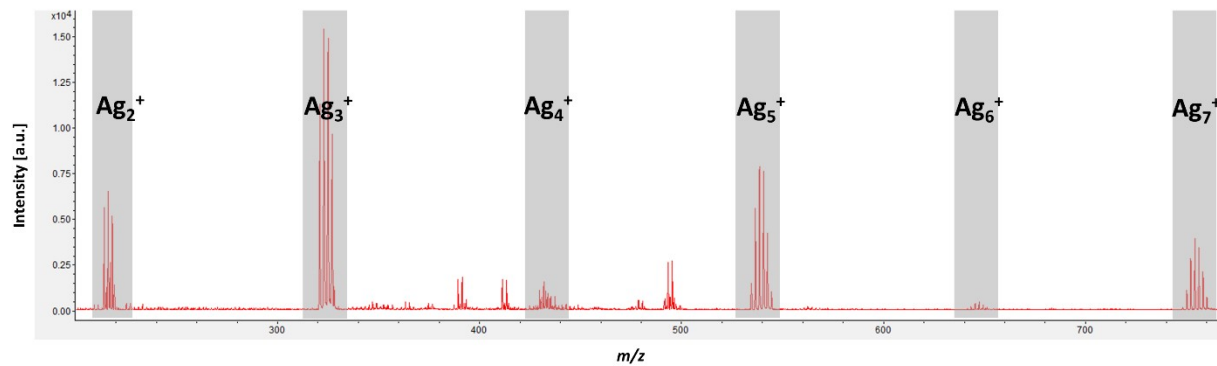
\*Correspondence to: Vladimír Vrkoslav (vladimir.vrkoslav@uochb.cas.cz), Institute of Organic Chemistry and Biochemistry of the Czech Academy of Sciences, Flemingovo nám. 542/2, Prague 6, 166 10, Czech Republic

**Supplementary Tab. 1.** Thermal evaporation settings.

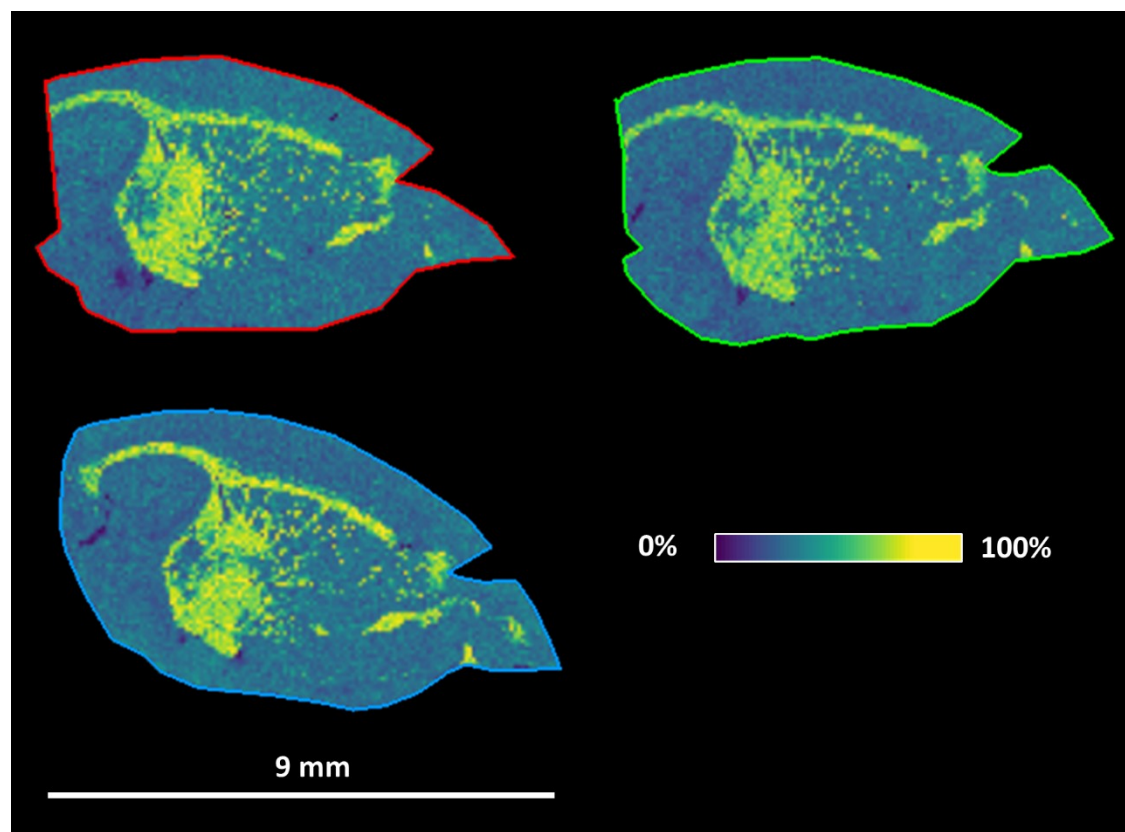
<b>Name</b>	<b>Value</b>	<b>Units</b>
Rise Time 1	00:30	mm:ss
Soak Power 1	10.0	%
Soak Time 1	00:30	mm:ss
Rise Time 2	00:30	mm:ss
Soak Power 2	15.0	%
Soak Time 2	00.20	mm:ss
Idle Ramp Time	00.30	mm:ss
Rate	5.000	Å/s
Final Thickness	0.060 or 0.11 or 0.22	kÅ
Thickness Set Point	0.060 or 0.11 or 0.22	kÅ
Control Gain	10	Å/s/%



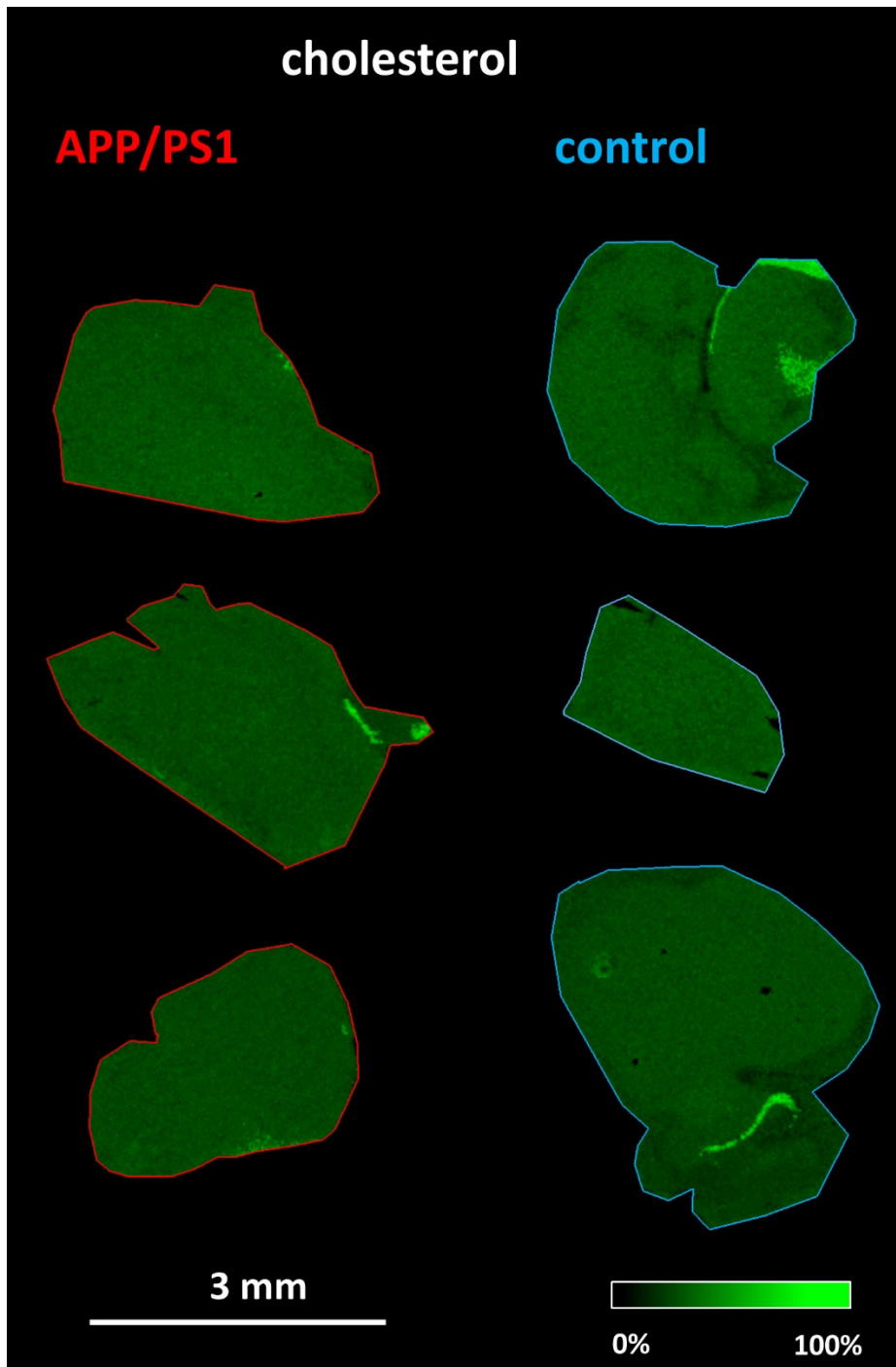
**Supplementary Fig. 1.** A) Ion yield and B) mass resolution plots as a function of laser intensity for different thicknesses of Ag. Cholesterol at  $m/z$  493.2  $[M + {}^{107}\text{Ag}]^+$ . Average of 5 spectra from AgLDI of a mouse brain cortex region.



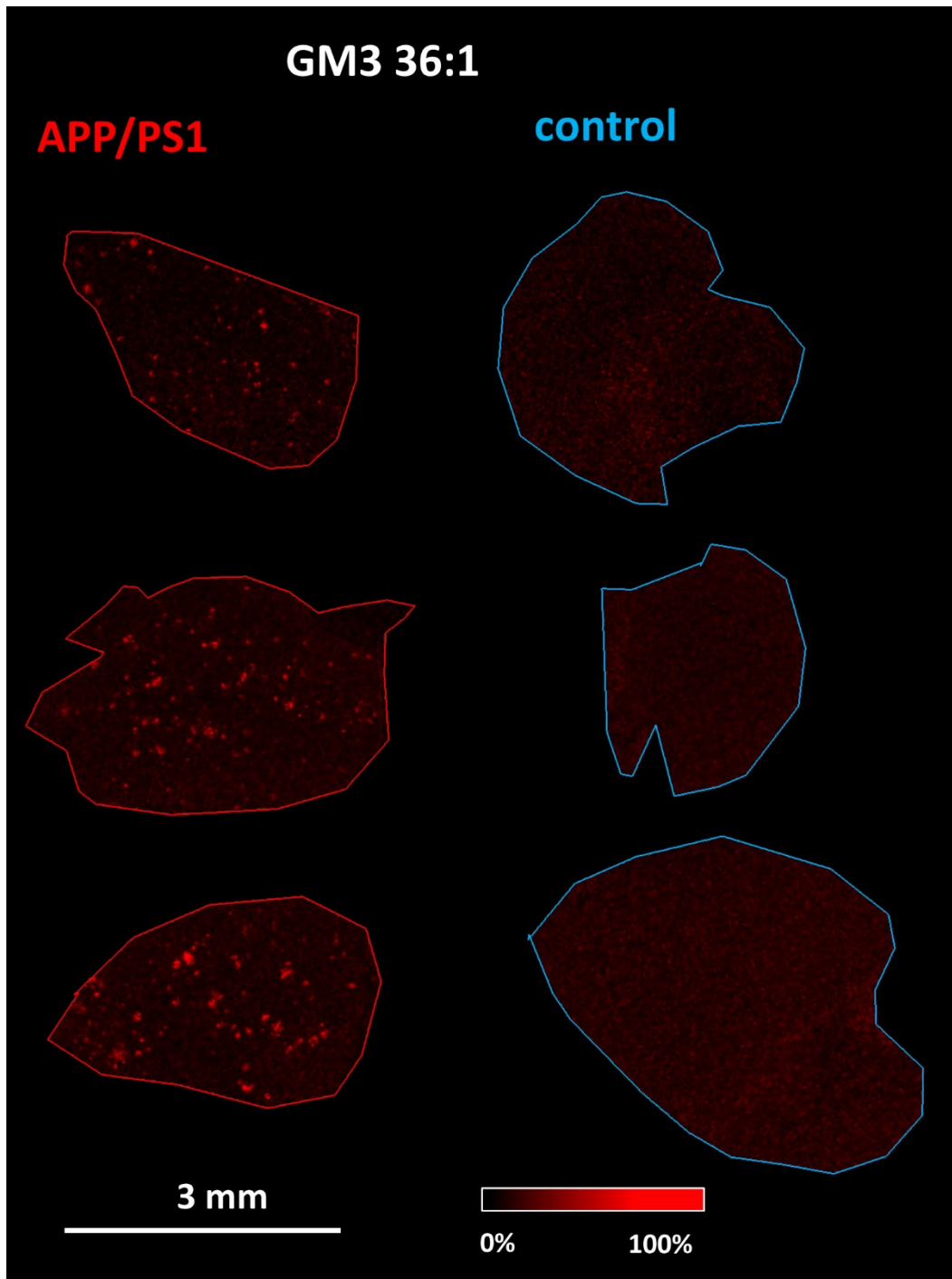
**Supplementary Fig. 2.** Representative spectra from AgLDI of a mouse brain section in the cortex region in positive ion mode. Section with Ag film with a thickness of 22 nm deposited using thermal evaporation showing various silver clusters.



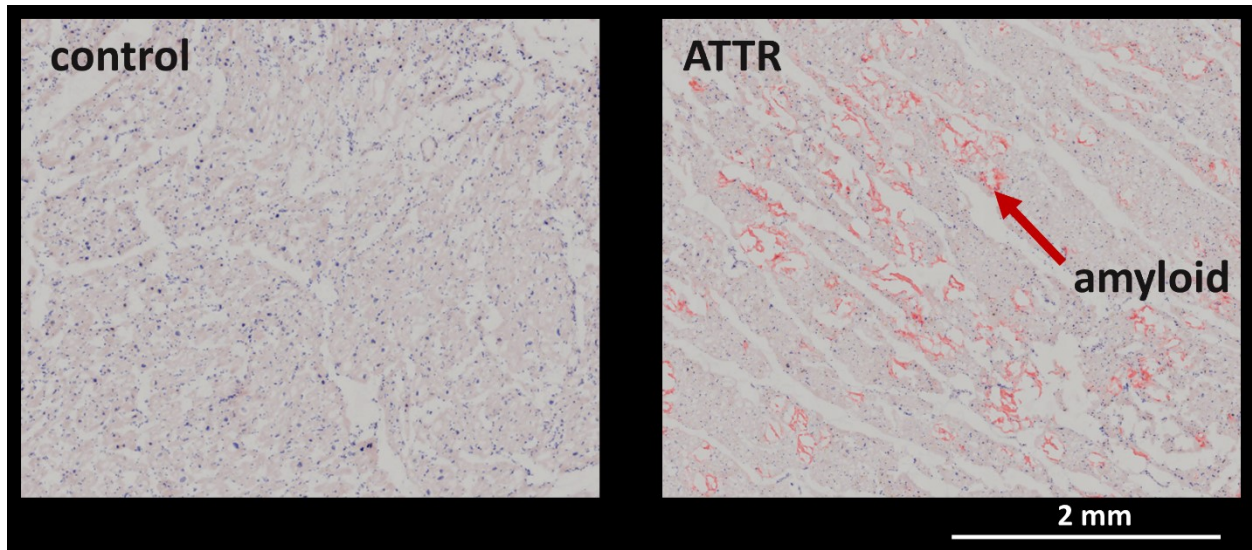
**Supplementary Fig. 3.** Reproducibility of the sample preparation process and analysis. AgLDI MSI (Ag 6 nm) of three consecutive sections of a single brain. Distribution of cholesterol at  $m/z$  493.2  $[M + {}^{107}\text{Ag}]^+$  using a spatial resolution of 70  $\mu\text{m}$ .



**Supplementary Fig. 4.** AgLDI MSI (Ag 6 nm) analysis of a frontal cortex section (APP/PS1 mice and age-matched WT controls). Ion images of cholesterol (green,  $m/z$  493.2,  $[M + {}^{107}\text{Ag}]^+$ ) at a spatial resolution of 20  $\mu\text{m}$ .

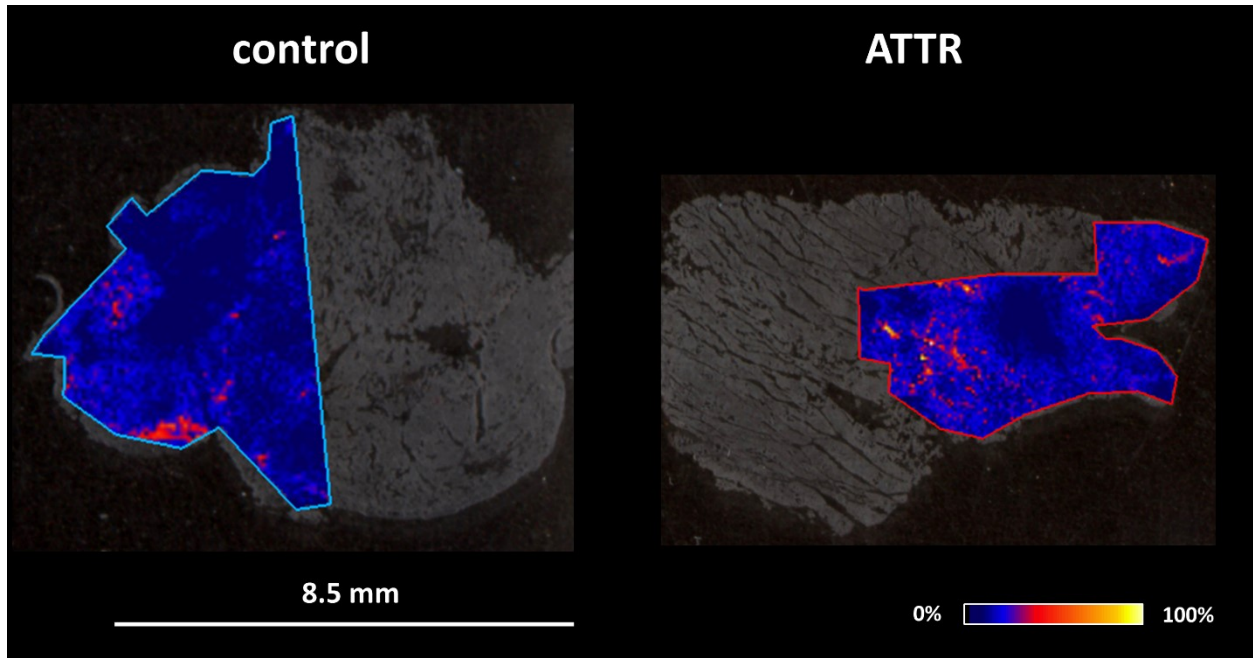


**Supplementary Fig. 5.** MALDI MSI (Ag 6 nm) analysis of a frontal cortex section (APP/PS1 mice and age-matched WT controls). Ion images of ganglioside (red,  $m/z$  1179.7 [M – H]<sup>-</sup>) at a spatial resolution of 20  $\mu$ m.

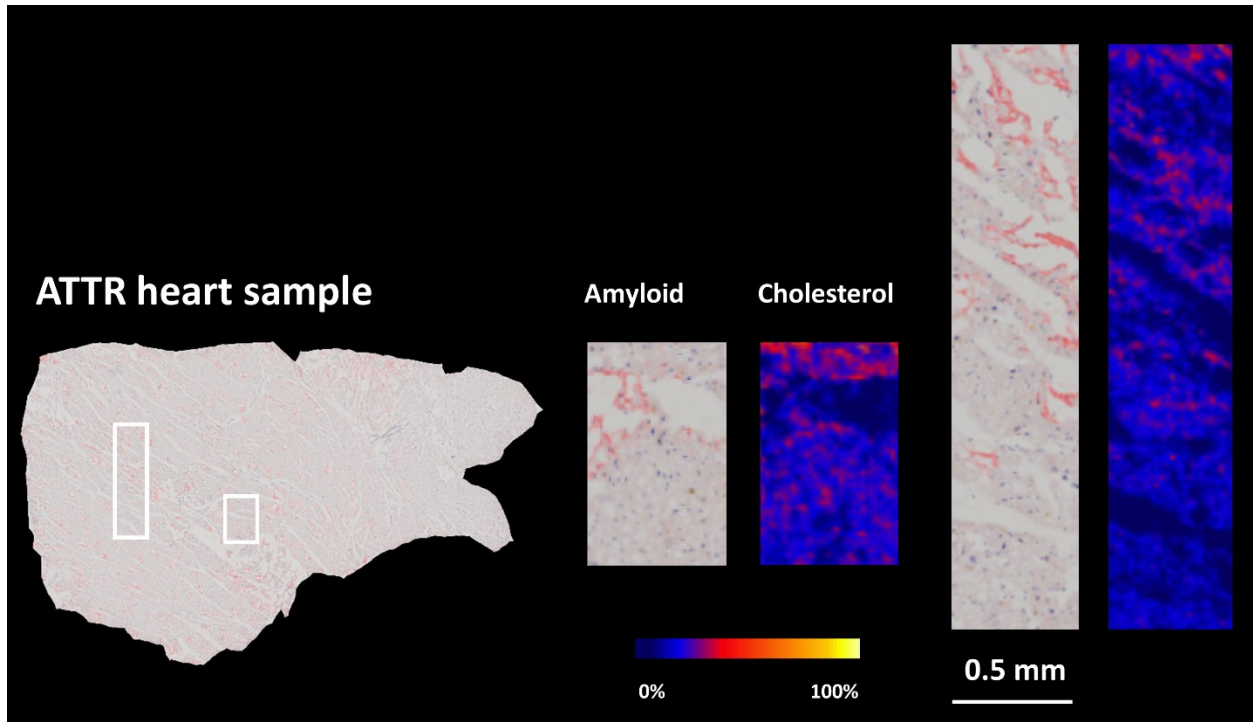


**Supplementary Fig. 6.** Congo red amyloid staining. Images of a control myocardial section (left) and an ATTR-affected myocardial section (right) under a light microscope.

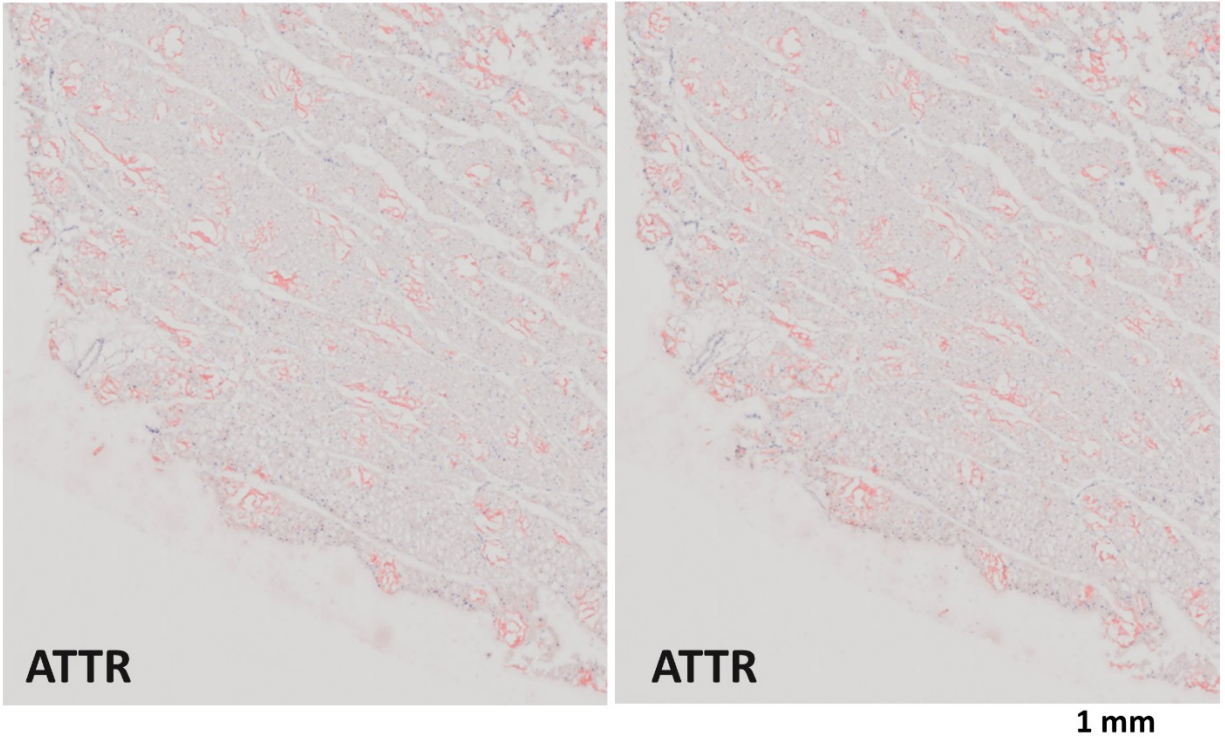




**Supplementary Fig. 7.** AgLDI MSI (Ag 6 nm) analysis of control (left) and ATTR-affected (right) myocardial section. Ion image cholesterol ( $m/z$  493.2,  $[M + {}^{107}\text{Ag}]^+$ ) at a spatial resolution of 20  $\mu\text{m}$ .



**Supplementary Fig. 8.** Congo red amyloid staining and AgLDI MSI (Ag 6 nm) analysis of ATTR-affected myocardial section. Ion image cholesterol ( $m/z$  493.2,  $[M + {}^{107}\text{Ag}]^+$ ) at a spatial resolution of 10  $\mu\text{m}$ .



**Supplementary Fig. 9.** Congo red amyloid staining. Images showing non-serial sections of an ATTR-affected myocardial section under a light microscope. The serial sections in between were analyzed by AgLDI.